Uncovering the Stabilization Mechanism in Bimetallic Ruthenium – Iridium Anodes for Proton Exchange Membrane Electrolyzers

*Viktoriia A. Saveleva[†], Li Wang[‡], Wen Luo[†], Spyridon Zafeiratos[†], Corinne Ulhaq-Bouillet[§], Aldo S. Gago[‡], K. Andreas Friedrich[‡], Elena R. Savinova[†]**

†Institut de Chimie et Procédés pour l'Energie, l'Environnement et la Santé, UMR 7515 du CNRS-UdS 25 Rue Becquerel, 67087 Strasbourg, France.

‡ Institute of Engineering Thermodynamics, German Aerospace Center (DLR), Pfaffenwaldring 38-40, 70569 Stuttgart, Germany

§Institut de Physique et Chimie des Matériaux de Strasbourg, 23 rue du Loess, BP 43, 67037, Strasbourg, France

Corresponding Author

*Corresponding author. Phone: ++33(0)3 68 85 27 39. Fax: ++33(0)3 68 85 27 61. E-mail: elena.savinova@unistra.fr

ABSTRACT. Proton exchange membrane (PEM) electrolyzers are attracting an increasing attention as a promising technology for the renewable electricity storage. In this work, near ambient pressure X-ray photoelectron spectroscopy (NAP-XPS) is applied for *in situ* monitoring

of the surface state of membrane electrode assemblies with RuO_2 and bimetallic $Ir_{0.7}Ru_{0.3}O_2$ anodes during water splitting. We demonstrate that Ir protects Ru from the formation of an unstable hydrous Ru(IV) oxide thereby rendering bimetallic Ru-Ir oxide electrodes with higher corrosion resistance. We further show that the water splitting occurs through a surface Ru(VIII) intermediate, and, contrary to common opinion, the presence of Ir does not hinder its formation.

TOC GRAPHICS

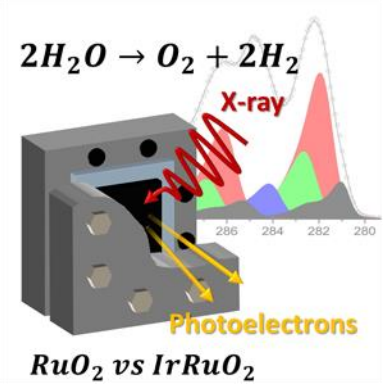

Water electrolysis via proton exchange membrane (PEM) cells is considered as the up-and-coming means for sustainable hydrogen production in the order of megawatts.[1] However, its efficiency is limited by the high overpotential of the oxygen evolution reaction (OER).[2,3] RuO_2 and IrO_2 are among the few most active electrode materials, which can withstand harsh acidic and oxidizing environment of the anode of a PEM electrolyzer, and have thus been the focus of detailed investigations (see [2,4–6] and Refs therein). However, the development of sufficiently stable anode materials with low OER overpotentials is still a challenge.

Various tools, such as electrochemical methods,[7–12] X-ray absorption spectroscopy,[3,13] as well as *ex situ* X-ray photoelectron spectroscopy (XPS),[7,14–17] have been applied to probe the state of Ir and Ru-based anodes and its dependence on the electrode potential. Already in the early studies, Kötz *et al.* proposed the OER mechanism involving changes in the red-ox states of Ru and Ir. However, this tentative mechanism has not been unambiguously confirmed yet.

While RuO_2 is more active and cheaper than IrO_2, it is prone to the electrochemical corrosion, which starts even before the OER onset[18] and prevents utilization of non-stabilized RuO_2 for large scale PEM electrolysis. Corrosion of Ru anodes was attributed to formation of soluble, volatile and poisonous Ru(VIII) compounds (supposedly RuO_4).[13,18,19]

Bimetallic anodes based on Ru and Ir oxides combine the catalytic activity of RuO_2 and the stability of IrO_2 and have thus attracted considerable attention.[2,4,16,20,21] On the basis of *ex situ* XPS and electrochemical studies, the Ir stabilization was proposed through a common valence band formation preventing RuO_4 generation.[21] Nevertheless, considering that RuO_4 could not be detected on the anode surface, the origin of the stabilizing influence of Ir is still uncertain.

Recent years have witnessed an increased interest[3,13,14,22–24] in Ru- and Ir-based anodes as oxygen evolution catalysts due to the increase of the share of renewable electricity in the energy mix and an ensuing strengthening of the R&D in the area of water electrolysis. However, the lack of the understanding of the Ir stabilization mechanism hinders the development of active and stable anode catalysts for PEM electrolyzers.

Thanks to its surface sensitivity and the capability to distinguish elements in various oxidation states, XPS has been widely applied to studies of mono- and bimetallic Ru(Ir) anodes after they were subjected to the OER.[16] However, conventional UHV-based XPS is insufficient to study the dynamic nature of interfacial processes. This limitation is overcome with the advent

of the so-called near-ambient-pressure XPS (NAP-XPS),[25] which has recently demonstrated its potential for *operando* investigations of electrocatalytic materials.[17,26–28]

In this work, we apply NAP-XPS and perform an *operando* investigation of membrane electrode assemblies (MEA) of a PEM electrolyzer with Ru/Ru-Ir oxide anodes to unveil the Ir stabilization effect during water splitting. Comprehensive analysis of XP spectra obtained in the presence of water vapor under electrochemical control allowed us to reveal formation of different valence states of Ru, follow their evolution with the electrode potential and shed light on the long-debated effect of Ir on the state of Ru.

Catalyst samples were prepared by direct reduction of Ru and Ir salts in water-free conditions, following a previously reported procedure[5] (Supporting Information I). Subsequent thermal treatment of the powders produced nanoparticles of rutile-type oxides with the particle size ranging from 8 to 90 and from 3 to 9 nm for RuO_2 and $Ir_{0.7}Ru_{0.3}O_2$, respectively (Figure 1 and Supporting Information II and III). Scanning transmission electron microscopy (STEM) measurements coupled with the EDX analysis revealed uniform distribution of Ir and Ru in $Ir_{0.7}Ru_{0.3}O_2$ suggesting formation of a single phase rather than a mixture of two separated RuO_2 and IrO_2 phases in the bimetallic sample.

Figure 2 compares the rotating disc electrode data for RuO_2 and $Ir_{0.7}Ru_{0.3}O_2$ anodes in 0.05 M H_2SO_4. In agreement with the literature data[14,15,23] the RuO_2 anode demonstrates noticeable OER activity already at 1.45 V vs. Reversible hydrogen electrode (RHE), which however rapidly decays upon potential cycling (Figure 2A) due to the electrode corrosion. Investigation of the degradation of Ru anodes has been subject of numerous publications in the past[9,14,18,19]. The $Ir_{0.7}Ru_{0.3}O_2$ anode shows a considerably slower decay of the OER currents above 1.45 V (Figure 2B and Figure S5B of the Supporting Information IV) confirming the higher stability of

bimetallic Ru(Ir) against monometallic Ru oxides documented in previous publications[10,16,21]. Similar (ca. 60 mV) Tafel slopes (Figure 2C) and overpotentials (Figure 2D) in the OER kinetic region (0.1 mA cm^{-2}) suggest the water splitting process on the Ru- and the Ru-Ir oxide electrode occur through the same rate-determining step. The Tafel slope for RuO_2 increases above 1.5 V *vs.* RHE, accounting for an additional kinetically unfavorable corrosion process and loss of material.

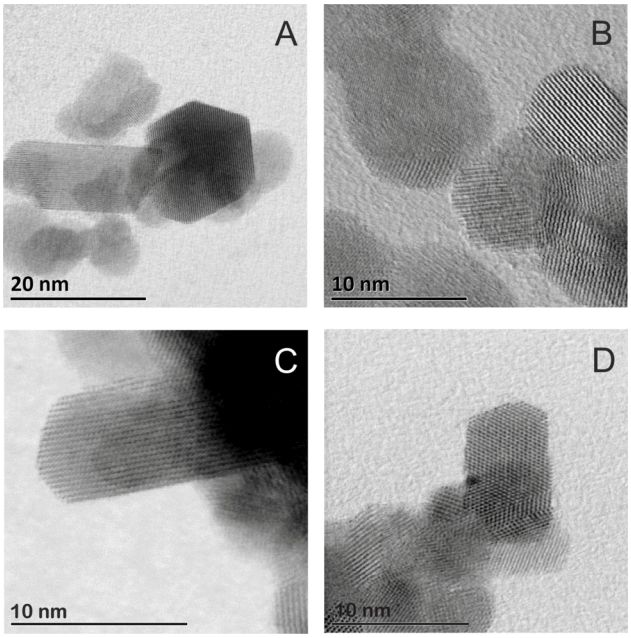

Figure 1. STEM images of RuO_2 (A,B) and $Ir_{0.7}Ru_{0.3}O_2$ (C,D) electrodes before (A,C) and after (B,D) the OER studies performed in the NAP-XPS chamber.

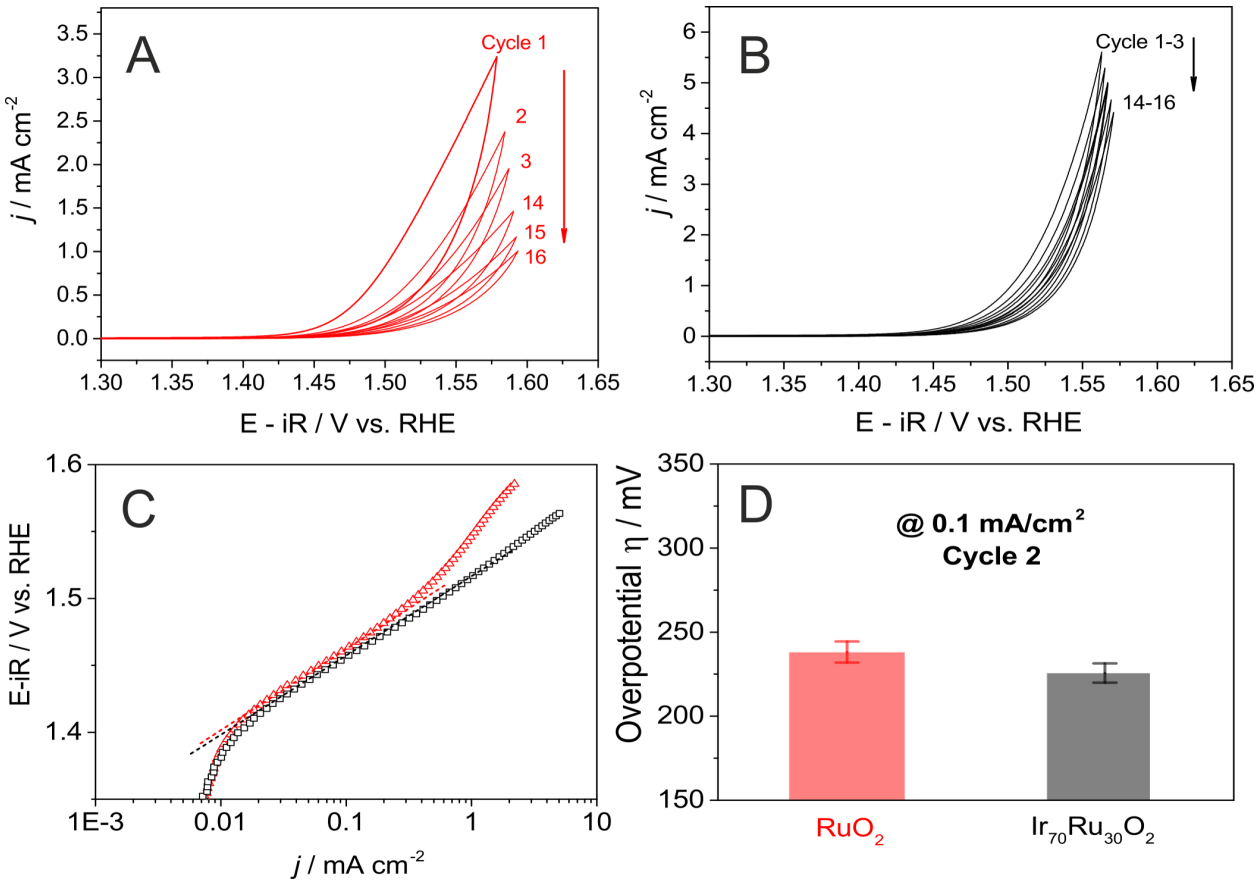

Figure 2. Current-potential characteristics of the RuO_2 (A), and the $Ir_{0.7}Ru_{0.3}O_2$ (B) anode measured in N_2-saturated 0.05 M H_2SO_4 at 25 °C with a scan rate of 5 mV s^{-1}; (C) Tafel plots constructed from the second current-potential scans and (D) overpotential at 0.1 mA cm^{-2}.

NAP-XPS measurements were performed using MEAs with RuO_2 and $Ir_{0.7}Ru_{0.3}O_2$ as the working electrodes (WEs) and commercial Pt/C as the counter electrode (CE). These were integrated in the electrochemical cell combined with the NAP-XPS spectrometer (see Supporting Information V, VI.1 and VI.2). While the e*x situ* characterization of the catalysts and the MEAs with STEM/EDX before and after operation did not reveal any noticeable structural or compositional changes resulting from the OER cycle (see Figure 1 and Supporting Information III), NAP-XPS measurements performed under 3 mbar of water and different electrode potentials

demonstrated significant dynamic changes underlining the importance of *in situ* investigation of the Ru-Ir anode under the OER conditions.

Figures 3 (A, B) show the Ru3d spectra of RuO_2 and $Ir_{0.7}Ru_{0.3}O_2$ electrodes exposed to a potential of 1.5 V, whereby the OER was confirmed by the mass spectrometer integrated in the measurement chamber (see Supporting Information VI.3). Four different states of Ru could be detected under the OER conditions, namely rutile-type RuO_2, hydrous Ru(IV) oxide $Ru(OH)_x$, as well as Ru in higher oxidation states (VI) and (VIII) (see the fitting procedure in Supporting Information VI.4).

Figures 3C and 3D demonstrate gradual transformation of the Ru(IV) oxide into other species for Ru- and Ru-Ir oxide electrodes as their potential is increased positive of 0 V. It is notable that Ru(VIII) species are detected at 1.0 V, i.e. below the standard potential of the RuO_4 phase formation (1.387 V[29]). This can be rationalized by the formation of either a thin surface layer or islands of $RuO_{4(s)}$ (rather than a RuO_4 phase), strongly interacting with the underlying $Ru(Ir)O_2$ substrate. The interaction of the overlayer with the substrate is likely to account for the potential shift from the thermodynamic value.[30]

While electrochemical formation of RuO_4 has been postulated in previous publications, it has never been detected on the anode surface either during or after the electrolysis, likely due to its instability at room temperature. Kötz *et al.* detected formation of dissolved corrosion products in the vicinity of the RuO_2 anode simultaneously with the OER and hypothesized on the RuO_4 generation and the OER occurring through common intermediates (Ru(VI) and Ru(VII) in the Kötz' scheme).[8]

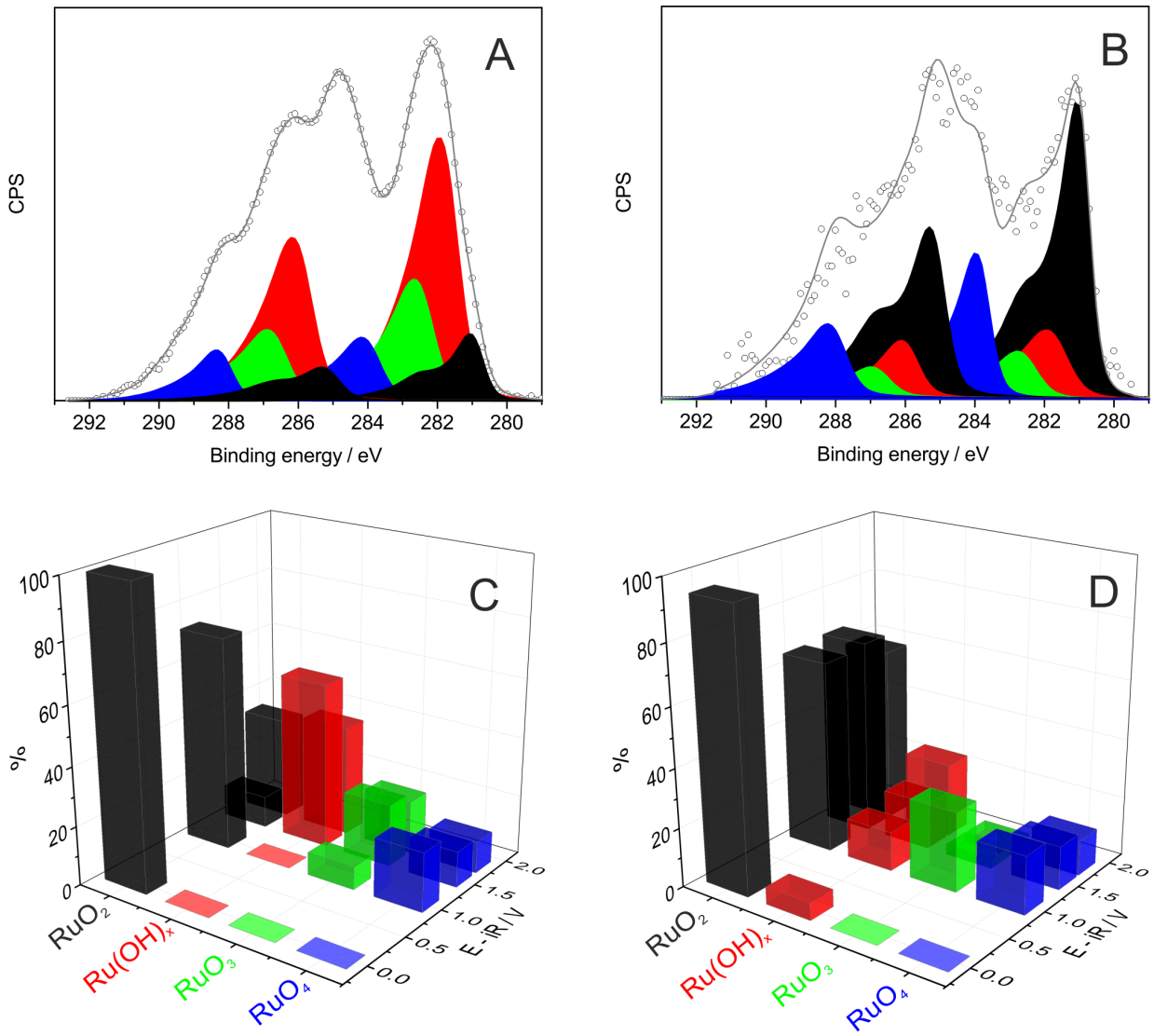

Figure 3. Upper panels: fitted C1s-Ru3d XP spectra of RuO_2 (A) and $Ir_{0.7}Ru_{0.3}O_2$ (B) electrodes at 1.5V. Experimental XPS data are shown as black cycles, fitted spectrum – as a grey line. For the sake of clarity carbon peaks are not shown. Bottom panels: Influence of the applied potential on the surface composition of RuO_2 (C) and $Ir_{0.7}Ru_{0.3}O_2$ (D) electrodes. Only forward scans are shown. Measurements were performed in 3 mbar H_2O ambient at a photon energy of 820 eV. The values of potential are iR corrected and are given on the dynamic hydrogen electrode (DHE) scale. Color codes: RuO_2 (black); $Ru(OH)_x$ (red); Ru(VI) abbreviated as RuO_3 (green); $RuO_{4(s)}$ (blue).

As the electrode potential is shifted positive, the contribution of $RuO_{4(s)}$ surface species declines (Figures 3C and D). This fact, along with the emergence of $RuO_{4(s)}$ below the OER onset, strongly suggests that $RuO_{4(s)}$ is generated in an electrochemical step (e.g. Eq 1) and acts as an intermediate in the OER. Evidence provided by the isotope labeling experiments[31,32] reinforced by the results of this work advocates the so-called lattice oxygen evolution reaction, whereby the OER results from the higher to lower oxide decomposition (Eq 2). [33]

$$RuO_2 + 2H_2O \rightarrow RuO_{4(s)} + 4H^+ + 4e^- \qquad \text{Eq. 1}$$

$$RuO_{4(s)} \rightarrow RuO_2 + O_2 \qquad \text{Eq. 2}$$

While previous studies, relying on either *ex situ* or indirect evidence, suggested that the stabilizing effect of Ir consisted in the inhibition of RuO_4 formation,[9,21] this work reveals that in contrast to the accepted opinion Ir does not attenuate the amount of $RuO_{4(s)}$ on the electrode surface. The latter acts as the OER intermediate and its contribution increases in the presence of Ir. Thus, we assume that the positive role of Ir does not consist in the inhibition of $RuO_{4(s)}$ formation but rather in its stabilization on the anode surface.

To further understand the role of Ir we turn the attention to the atomic contributions of rutile-type anhydrous RuO_2 and hydrous $Ru(OH)_x$ oxide. One may notice that a significant growth of $Ru(OH)_x$ starts at the OER onset potential, and this effect is especially important for the monometallic RuO_2 electrode. The presence of Ir does not completely exclude the surface hydration, but limits its level at ca. 20%. Moreover, the potential reversal results in the virtual restoration of the initial composition for $Ir_{0.7}Ru_{0.3}O_2$ (cf. Figure S11B in the Supporting

Information). Conversely, the contribution of the hydrated phase to the monometallic RuO_2 electrode does not descend but continuously increases upon potential cycling suggesting the irreversibility of the anhydrous-to-hydrous oxide transition (Figures S11B and S12 in the Supporting Information). We thus conclude that $Ru(OH)_x$ is formed as a result of the catalytic OER cycle. We suggest that the main role of Ir lies in stabilizing Ru in the form rutile-type phase, preventing its irreversible transformation into a less stable hydroxide form, which is prone to corrosion. The effect of the surface hydration on the activity of IrRu-based catalysts has been discussed previously,[10] but not yet unequivocally confirmed.

As to the Ru(VI) species, which in the literature is often denoted as RuO_3, it shows up at 1 V, simultaneously with $RuO_{4(s)}$, its contribution above the OER onset decreasing with the electrode potential for the $Ir_{0.7}Ru_{0.3}O_2$ and increasing for the RuO_2 electrode (cf. Figure 3C and 3D). Moreover, the RuO_3 component persists on the RuO_2 electrode even upon the reversal of the voltage bias (Supporting Information VI.6 and VI.7). Such a behavior suggests that in contrast to the accepted opinion (see recent review[2] and references therein) RuO_3 is not the OER intermediate and that the decrease of its coverage on the $Ir_{0.7}Ru_{0.3}O_2$ against the RuO_2 anode is related to the increased stability of the former.

Figure 4 represents the Ru3d XP spectra acquired at two different photon energies (820 and 1300 eV corresponding to the penetration depth of 3.7 and 5.2 nm respectively) and two different potentials (data at other potentials are shown in the Supporting Information VI.5). We conclude that the core of the particles largely consists of an anhydrous Ru(Ir) rutile-type oxide, while Ru(IV) hydroxide as well as $RuO_{4(s)}$ and RuO_3 components are present at the surface, confirming that the processes investigated in this work are interface-localized.

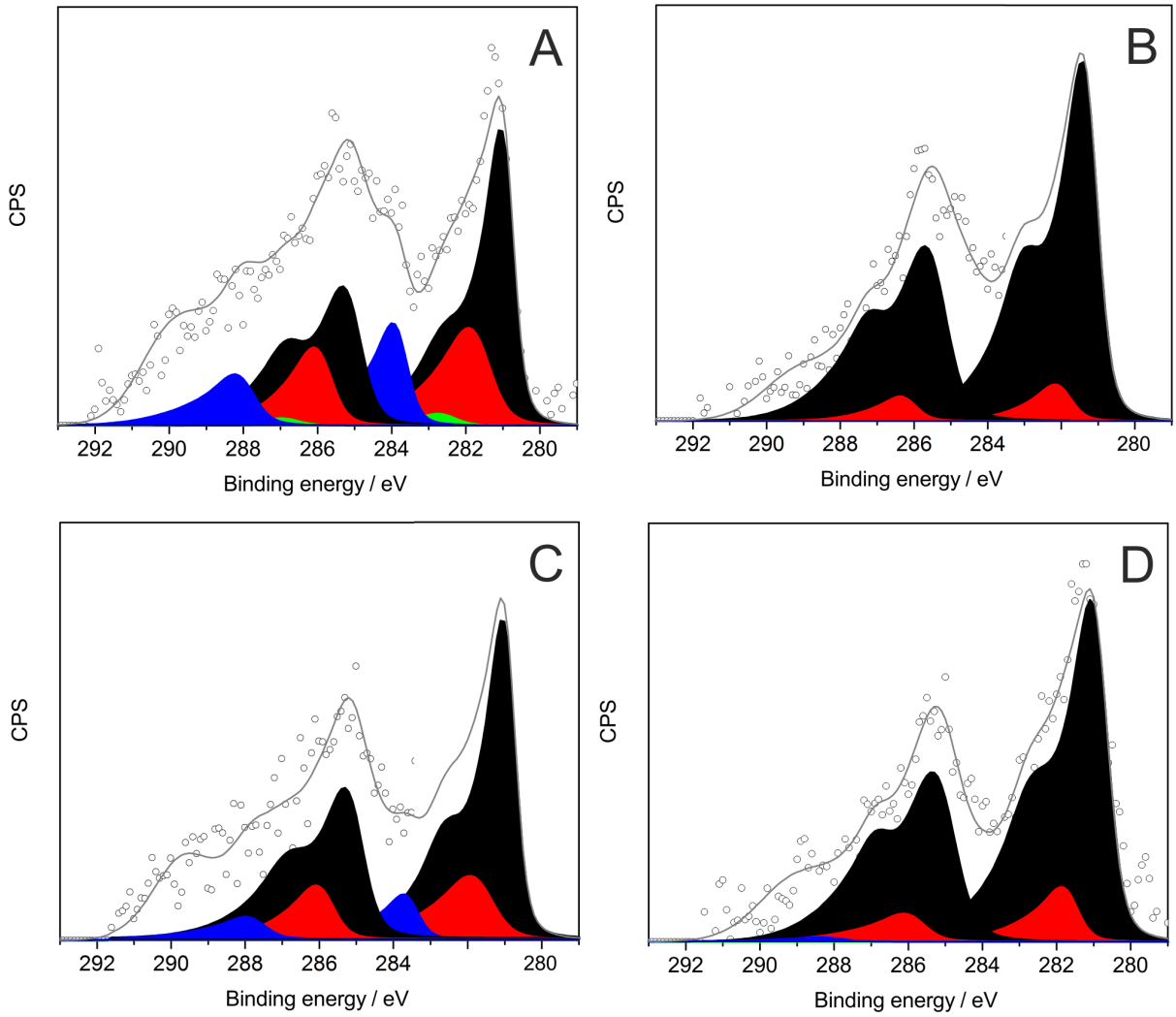

Figure 4. Ru3d spectra of $Ir_{0.7}Ru_{0.3}O_2$ electrode in 3 mbar H_2O ambient under 1.8V (A,B) and 2.5V (C,D) at different photon energies: 820eV (A,C) and 1300eV (B,D). Experimental XPS data are shown as black cycles, fitted spectrum – as a grey line. For the sake of clarity carbon peaks are not shown. Color codes: RuO_2 (black); $Ru(OH)_x$ (red); Ru(VI) abbreviated as RuO_3 (green); $RuO_{4(s)}$ (blue).

In contrast to Ru3d, Ir4f XP spectra did not show any change under the polarization in contrast with the previous *in situ* studies of a monometallic IrO_2 anode[17], and Ir sites were represented by a Ir(IV) rutile-type oxide throughout the experiment and regardless the electrode

potential (Figure S13 of the Supporting Information). Various hypotheses may be put forward to explain this observation. Thus, the Ir rutile-type oxide may serve as a matrix stabilizing the more active Ru sites, whereby the OER preferentially occurs. Alternatively, the surface concentration of Ir in higher oxidation state(s) may be too small preventing their detection, or the OER on the Ir oxide occurs via a mechanism, which involves an anion- rather than the cation red-ox cycle as recently documented in refs[34,35]. Meanwhile, the Ir/Ru atomic ratio increased with the applied potential (cf. Figure S14 in the Supporting Information), confirming the Ir surface enrichment in the OER region also documented in previous studies.[15,16] The observed increase of the Ir/Ru atomic ratio with the applied potential may be attributed to the loss of Ru, which may either occur via partial dissolution of the Ru(VIII) species in the liquid phase (electrolysis in a liquid electrolyte or in a membrane-electrode assembly in contact with liquid water) or their sublimation into the gas phase (this work).

In conclusion, we have discovered a new degradation mechanism of Ru-Ir anodes by analyzing *in situ* the surface oxidation states of PEM electrolyzer MEAs, operating at near ambient pressure. Our study reveals significant potential-dependent changes in the valence state as well as the degree of hydration of Ru, which cannot be detected using *ex situ* methods. We demonstrate that under operation rutile-type RuO_2 anodes gradually and irreversibly transform into a hydrous Ru(IV) oxide form, while Ir stabilizes Ru in the anhydrous rutile phase. We point out that $RuO_{4(s)}$ surface oxide is formed on the anode surface and acts as the OER intermediate. The presence of Ir does not reduce the surface coverage of the $RuO_{4(s)}$ oxide but rather stabilizes it on the surface. By tuning the photon energy we show that the core of the catalytic particles mainly consists from an anhydrous Ru-Ir(IV) oxide phase, while the surface is represented by the Ir(IV) oxide, hydrated form of Ru(IV) oxide and Ru in higher valence states, namely RuO_3 and

$RuO_{4(s)}$. We finally conclude that the Ir stabilization mechanism consists in protecting RuO_2 from its irreversible transformation into either the unstable hydrous Ru(IV) oxide phase or RuO_3, and in stabilizing the $RuO_{4(s)}$ intermediate on the anode surface against its dissolution (sublimation). The results presented herein suggest that stabilization of Ru in the rutile oxide against the hydroxide phase is a clue to the development of stable Ru-based anodes for PEM electrolyzers.

Supporting Information (PDF). Catalyst preparation, X-ray powder diffraction, Transmission electron microscopy, Electrochemical measurements of the sample in 0.05M H_2SO_4, Preparation of MEAs for NAP-XPS measurements, NAP-XPS measurements (experimental protocol, electrochemical characterization of the MEAs in the NAP-XPS chamber, online mass spectrometry in the NAP-XPS chamber, C1sRu3d XP spectra peak fitting procedure, potential dependence of Ru components for the $Ir_{0.7}Ru_{0.3}O_2$ sample at two different photon energies, potential dependence of Ru components for RuO_2 and $Ir_{0.7}Ru_{0.3}O_2$ electrodes in a backward scan, influence of repetitive potential cycles on the composition of the RuO_2 electrode, Ir4f XP spectra peak fitting, Ir/Ru atomic ratio as a function of the electrode potential)

ACKNOWLEDGMENT

The authors acknowledge the EU FP7/2007-2013 for Fuel Cell and Hydrogen Joint Technology Initiative under Grant No. 621237 (INSIDE) for the financial support. We thank T. Dintzer (Strasbourg, France) for SEM measurements, R. Schloegl, A. Knop-Gericke and M. Hävecker (FHI der MPG, Berlin, Germany) for the opportunity to use ISISS beamline, and HZB for the allocation of the synchrotron radiation beamtime.

REFERENCES

(1) Friedrich, K. A. *PlanDelyKad Study on Large Scale Water Electrolysis and Hydrogen Storage, German Federal Ministry for Economic Affairs and Energy (BMWi)*; 2015.

(2) Fabbri, E.; Habereder, A.; Waltar, K.; Kötz, R.; Schmidt, T. J. Developments and Perspectives of Oxide-Based Catalysts for the Oxygen Evolution Reaction. *Catal. Sci. Technol.* **2014**, *4*, 3800–3821.

(3) Katsounaros, I.; Cherevko, S.; Zeradjanin, A. R.; Mayrhofer, K. J. J. Oxygen Electrochemistry as a Cornerstone for Sustainable Energy Conversion. *Angew. Chemie - Int. Ed.* **2014**, *53*, 102–121.

(4) Matsumoto, Y.; Sato, E. Electrocatalytic Properties of Transition Metal Oxides for Oxygen Evolution Reaction. *Mater. Chem. Phys.* **1986**, *14*, 397–426.

(5) Lettenmeier, P.; Wang, L.; Golla-Schindler, U.; Gazdzicki, P.; Cañas, N. A.; Handl, M.; Hiesgen, R.; Hosseiny, S. S. S.; Gago, A. S.; Friedrich, A. K. Nanosized IrOx-Ir Catalyst with Relevant Activity for Anodes of PEM Electrolysis Produced by a Cost-Effective Procedure. *Angew. Chemie* **2015**, *128*, 752–756.

(6) Reier, T.; Pawolek, Z.; Cherevko, S.; Bruns, M.; Jones, T.; Teschner, D.; Selve, S.; Bergmann, A.; Nong, H. N.; Schlögl, R.; et al. Molecular Insight in Structure and Activity of Highly Efficient, Low-Ir Ir-Ni Oxide Catalysts for Electrochemical Water Splitting (OER). *J. Am. Chem. Soc.* **2015**, *137*, 13031–13040.

(7) Peuckert, M. XPS Study on Thermally and Electrochemically Prepared Oxidic Adlayers on Iridium. *Surf. Sci. Lett.* **1984**, *144*, 451–464.

(8) Kötz, R.; Lewerenz, H. J.; Brüesch, P.; Stucki, S. Oxygen Evolution on Ru and Ir Electrodes. *J. Electroanal. Chem. Interfacial Electrochem.* **1983**, *150*, 209–216.

(9) Kötz, R.; Stucki, S.; Scherson, D.; Kolb, D. M. In-Situ Identification of RuO4 as the Corrosion Product During Oxygen Evolution on Ruthenium in Acid Media. *J. Electroanal. Chem.* **1984**, *172*, 211–219.

(10) Lyons, M. E. G.; Floquet, S. Mechanism of Oxygen Reactions at Porous Oxide Electrodes. Part 2—Oxygen Evolution at RuO2, IrO2 and IrxRu1−xO2 Electrodes in Aqueous Acid and Alkaline Solution. *Phys. Chem. Chem. Phys.* **2011**, *13*, 5314–5355.

(11) Miles, M. H.; Klaus, E. A.; Gunn, B. P.; Locker, J. R.; Serafin, W. E.; Srinivasan, S. The Oxygen Evolution Reaction on Platinum, Iridium, Ruthenium and Their Alloys at 80°C in Acid Solutions. *Electrochim. Acta* **1978**, *23*, 521–526.

(12) Alia, S. M.; Pylypenko, S.; Neyerlin, K. C.; Kocha, S. S.; Pivovar, B. S. Activity and Durability of Iridium Nanoparticles in the Oxygen Evolution Reaction Shaun M. Alia,. *ECS Trans.* **2015**, *69*, 883–892.

(13) Danilovic, N.; Subbaraman, R.; Chang, K. C.; Chang, S. H.; Kang, Y.; Snyder, J.; Paulikas, A. P.; Strmcnik, D.; Kim, Y. T.; Myers, D.; et al. Using Surface Segregation to Design Stable Ru-Ir Oxides for the Oxygen Evolution Reaction in Acidic Environments. *Angew. Chem. Int. Ed. Engl.* **2014**, *53*, 14016–14021.

(14) Paoli, E. A.; Masini, F.; Frydendal, R.; Deiana, D.; Schlaup, C.; Malizia, M.; Hansen, T. W.; Horch, S.; Stephens, I. E. L.; Chorkendorff, I. Oxygen Evolution on Well-Characterized Mass-Selected Ru and RuO_2 Nanoparticles. *Chem. Sci.* **2015**, *6*, 190–196.

(15) Owe, L. E.; Tsypkin, M.; Wallwork, K. S.; Haverkamp, R. G.; Sunde, S. Iridium-Ruthenium Single Phase Mixed Oxides for Oxygen Evolution: Composition Dependence of Electrocatalytic Activity. *Electrochim. Acta* **2012**, *70*, 158–164.

(16) Angelinetta, C.; Trasatti, S.; Atanososka, L. D.; Atanasoski, R. T. Surface Properties of RuO2 + IrO2 Mixed Oxide Electrodes. *J. Electroanal. Chem. Interfacial Electrochem.* **1986**, *214*, 535–546.

(17) Sanchez Casalongue, H. G.; Ng, M. L.; Kaya, S.; Friebel, D.; Ogasawara, H.; Nilsson, A. In Situ Observation of Surface Species on Iridium Oxide Nanoparticles during the Oxygen Evolution Reaction. *Angew. Chem. Int. Ed. Engl.* **2014**, *53*, 7169–7172.

(18) Hodnik, N.; Jovanovič, P.; Pavlišič, A.; Jozinović, B.; Zorko, M.; Bele, M.; Šelih, V. S.; Šala, M.; Hočevar, S.; Gaberšček, M. New Insights into Corrosion of Ruthenium and Ruthenium Oxide Nanoparticles in Acidic Media. *J. Phys. Chem. C* **2015**, *119*, 10140–10147.

(19) Iwakura, C.; Hirao, K.; Tamura, H. Anodic Evolution of Oxygen on Ruthenium in Acidic Solutions. *Electrochim. Acta* **1977**, *22*, 329–334.

(20) Over, H. Surface Chemistry of Ruthenium Dioxide in Heterogeneous Catalysis and Electrocatalysis: From Fundamental to Applied Research. *Chem. Rev.* **2012**, *112*, 3356–3426.

(21) Kötz, R.; Stucki, S. Stabilization of RuO2 by IrO2 for Anodic Oxygen Evolution in Acid Media. *Electrochim. Acta* **1986**, *31*, 1311–1316.

(22) Sardar, K.; Petrucco, E.; Hiley, C. I.; Sharman, J. D. B.; Wells, P. P.; Russell, A. E.; Kashtiban, R. J.; Sloan, J.; Walton, R. I. Water-Splitting Electrocatalysis in Acid Conditions Using Ruthenate-Iridate Pyrochlores. *Angew. Chemie - Int. Ed.* **2014**, *53*, 10960–10964.

(23) Stoerzinger, K. A.; Qiao, L.; Biegalski, M. D.; Shao-Horn, Y. Orientation-Dependent Oxygen Evolution Activities of Rutile IrO 2 and RuO 2. *J. Phys. Chem. Lett.* **2014**, *5*, 1636–1641.

(24) Rossmeisl, J.; Qu, Z. W.; Zhu, H.; Kroes, G. J.; Nørskov, J. K. Electrolysis of Water on Oxide Surfaces. *J. Electroanal. Chem.* **2007**, *607*, 83–89.

(25) Salmeron, M.; Schlögl, R. Ambient Pressure Photoelectron Spectroscopy: A New Tool for Surface Science and Nanotechnology. *Surf. Sci. Rep.* **2008**, *63*, 169–199.

(26) Law, Y. T.; Zafeiratos, S.; Neophytides, S. G.; Orfanidi, A.; Costa, D.; Dintzer, T.; Arrigo, R.; Gericke, K.; Schlögl, R.; Savinova, E. R. In Situ Investigation of Dissociation and Migration Phenomena at the Pt / Electrolyte Interface of an Electrochemical Cell. *Chem. Sci.* **2015**, *6*, 5635–5642.

(27) Saveleva, V. A.; Papaefthimiou, V.; Daletou, M. K.; Doh, W. H.; Ulhaq-Bouillet, C.; Diebold, M.; Zafeiratos, S.; Savinova, E. R. *Operando* Near Ambient Pressure XPS (NAP-XPS) Study of the Pt Electrochemical Oxidation in H_2O and H_2O/O_2 Ambients. *J. Phys. Chem. C* **2016**, DOI: 10.1021/acs.jpcc.5b12410.

(28) Arrigo, R.; Hävecker, M.; Schuster, M. E.; Ranjan, C.; Stotz, E.; Knop-Gericke, A.; Schlögl, R. In Situ Study of the Gas-Phase Electrolysis of Water on Platinum by NAP-

XPS. *Angew. Chemie - Int. Ed.* **2013**, *52*, 11660–11664.

(29) Pourbaix, M. J. N.; Van Muylder, J.; de Zoubov, N. Electrochemical Properties of the Platinum Metals - Johnson Matthey Technology Review. *Platin. Met. Rev.* **1959**, *3*, 100–106.

(30) Campbell, C. T. Transition Metal Oxides: Extra Thermodynamic Stability as Thin Films. *Phys. Rev. Lett.* **2006**, *96*, 066106(1) – 066106(4).

(31) Wohlfahrt-Mehrens, M.; Heitbaum, J. Oxygen Evolution on Ru and RuO 2 Electrodes Studied Using Isotope Labelling and on-Line Mass Spectrometry. *J. Electroanal. Chem. Interfacial Electrochem.* **1987**, *237*, 251–260.

(32) Fierro, S.; Nagel, T.; Baltruschat, H.; Comninellis, C. Investigation of the Oxygen Evolution Reaction on Ti/IrO2 Electrodes Using Isotope Labelling and on-Line Mass Spectrometry. *Electrochem. commun.* **2007**, *9*, 1969–1974.

(33) Binninger, T.; Mohamed, R.; Waltar, K.; Fabbri, E.; Levecque, P.; Kötz, R.; Schmidt, T. J. Thermodynamic Explanation of the Universal Correlation between Oxygen Evolution Activity and Corrosion of Oxide Catalysts. *Sci. Rep.* **2015**, *5*, 12167–1213.

(34) Grimaud, A.; Hong, W. T.; Shao-Horn, Y.; Tarascon, J.-M. Anionic Redox Processes for Enhanced Battery and Water Splitting Devices. *Nat. Mater.* **2016**, *15*, 121–126.

(35) Mueller, D. N.; Machala, M. L.; Bluhm, H.; Chueh, W. C. Redox Activity of Surface Oxygen Anions in Oxygen-Deficient Perovskite Oxides during Electrochemical Reactions. *Nat. Commun.* **2015**, *6*, 6097–6105.